CHEMPHYSCHEM

ChemPubSoc Europe

DOI: 10.1002/cphc.201101000

Engineering the Atomic Structure of Carbon Nanotubes by a Focused Electron Beam: New Morphologies at the Sub-Nanometer Scale

Julio A. Rodríguez-Manzo,[a, b] Arkady V. Krasheninnikov,[c] and Florian Banhart*[a]

Carbon atoms are displaced in pre-selected locations of carbon nanotubes by using a focused electron beam in a scanning transmission electron microscope. Sub-nanometer-sized holes are created that change the morphology of double and triple-walled carbon nanotubes and connect the shells in a unique way. By combining in situ transmission electron microscopy experiments with atomistic simulations, we study the bonding between defective shells in the new structures which are reminiscent of the shape of a flute. We demonstrate that in double-walled nanotubes the shells locally merge by forming nanoarches while atoms with dangling bonds can be preserved in triple-walled carbon nanotubes. In the latter system, nanoarches are formed between the inner- and outermost shells, shielding small graphenic islands with open edges between the neighboring shells. Our results indicate that arrays of quantum dots may be produced in carbon nanotubes by spatially localized electron irradiation, generating atoms with dangling bonds that may give rise to localized magnetic moments.

1. Introduction

Numerous experiments have demonstrated that irradiation of nanostructures with energetic particles, especially when combined with heat treatment of the sample, give rise to atomic-scale defects but may also have overall beneficial effects on the sample (see refs. [1–3] for an overview). This is particularly relevant to carbon nanomaterials such as graphene, carbon nanotubes (CNTs) and fullerenes. Specifically, irradiation treatment of the CNTs can give rise to enhanced field emission[4,5] and an increase in the CNT film conductance.[6,7] Mechanical strengthening of CNT bundles,[8,9] multi-walled nanotubes (MWNTs),[10] and bulk CNT samples[7,11,12] due to irradiation-induced defects has been reported. CNTs can be welded together by irradiation[13–16] or connected to a metal.[17,18] Intentional introduction of defects[19] into graphene by irradiation has recently been demonstrated to be a powerful tool for engineering the atomic and electronic structure of graphene[20–23] or decorating these systems with metal atoms.[24,25] Moreover, many fascinating irradiation-induced phenomena in carbon nanomaterials inherently related to their nanometer size have been reported, such as pressure build-up inside irradiated carbon onions[26] and CNTs.[27,28]

The constructive role of electron irradiation in a transmission electron microscope (TEM) has been particularly emphasized, as the electron beam makes it possible not only to change the atomic structure of the system but also provides in situ information on the evolution of the system during exposure to the beam and thus at least partial control over the process. Electron irradiation with energies exceeding the threshold[29–32] for displacing carbon atoms ballistically (the threshold can be defined as the minimum electron energy required to knock out a carbon atom due to direct impact) has been demonstrated to give rise to the development of holes in graphene[20,33] and CNTs,[34] while irradiation with electron energies below the threshold can stimulate structural defects due to bond rotation.[20,35]

Here, using a focused electron beam in a scanning transmission electron microscope (STEM), we create a number of neighboring holes along the nanotube and change the morphology of double- (DWNTs) and triple-walled carbon nanotubes (TWNTs). By combining STEM experiments with atomistic simulations, we further study the bonding between the shells in the modified structures. We demonstrate that while in DWNTs the shells locally merge together by forming nanoarches as in double-layer graphene[36] and graphite,[37] the atoms with dangling bonds can be preserved in the TWNTS and are shielded by the nanoarches formed by the atoms in the outermost and innermost shells. As atoms with dangling bonds normally give rise to localized magnetic moments, our results indicate that

[a] Dr. J. A. Rodríguez-Manzo, Prof. F. Banhart
Institut de Physique et Chimie des Matériaux
University of Strasbourg
UMR 7504 CNRS, 23 rue du Loess
67034 Strasbourg (France)
E-mail: Banhart@ipcms.u-strasbg.fr

[b] Dr. J. A. Rodríguez-Manzo
Department of Physics and Astronomy
University of Pennsylvania
Philadelphia, Pennsylvania 19104 (USA)

[c] Dr. A. V. Krasheninnikov
Department of Physics, University of Helsinki
P.O. Box 43, FI-00014 (Finland)
and
Department of Applied Physics
Aalto University, P.O. Box 11100
FI-00076 Aalto (Finland)

arrays of magnetic quantum dots may potentially be produced in CNTs by spatially localized electron irradiation.

2. In situ STEM Experiments

Our experiments were carried out using an STEM (JEOL 2100F) equipped with a corrector for the spherical aberration, allowing us to focus the electron beam down to a spot of ~1 Å in diameter. The STEM was operated at 200 kV, producing electrons with sufficient energy to displace carbon atoms in the lattice.[29] Samples of carbon nanotubes with different number of layers (Thomas Swan & Co. Ltd.) were dispersed in ethanol. A drop of the dispersion was placed on a Cu TEM grid. For observation, the samples were mounted in a heating TEM holder (Gatan Ltd.), allowing imaging and irradiation of the sample in the microscope in a wide temperature range at vacuum conditions of ~10^{-5} Pa.

A standard experiment consisted in finding a DWNT or a TWNT next to a bundle to increase the stability under irradiation and prevent buckling. Then, the condensed electron beam was directed onto specific regions of the chosen nanotube (as shown in Figure 1), allowing the desired transformation. In this way, a series of sub-nanometer holes, with interdistances of less than two nanometers, were routinely achieved. Given the size of the electron beam (~1 Å), the incision size was dictated by the stability of the surrounding carbon lattice as well as the number of layers in the nanotube. All of our experiments were performed at 500 °C to increase the mobility of point defects and to avoid their clustering.[1] During the exposure to the electron beam, the damage in other parts of the nanotubes was minimal (grade 1, according to the universal damage grade table[38] in CNTs).

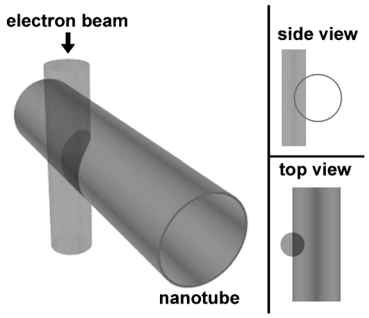

Figure 1. Setup of the experiments: The microscope is operated in the scanning transmission mode. The beam direction is perpendicular to the nanotube axis. The electron beam is focused onto the side region of the tube.

Figure 2 shows the consecutive formation of holes in a DWNT. The DWNT (Figure 2a) lies on the outer part of a nanotube bundle, which serves both as a support and reference frame throughout the STEM irradiation experiments. After the beam has been focused onto a specific region of the DWNT, a hole appears (Figure 2b). The details of the regions are shown in the inset of Figure 2b. Atoms with dangling bonds form interlayer links and lead to a slight distortion of the structure. Figure 2c shows another incision that has been made approximately three nanometers away from the first one. The two holes (marked with white arrows) induce an interaction between the inner and outer shells of the DWNT in the middle region (shown in the inset). The process can easily be extended, as evident from Figure 2d, where four additional holes were made at roughly the same spacing.

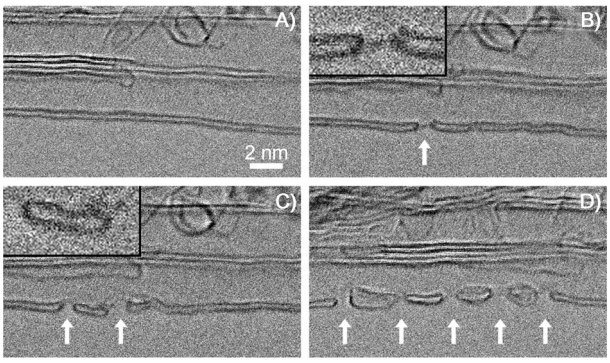

Figure 2. Electron-beam-induced formation of holes in a DWNT: A) pristine DWNT before irradiation. Formation of one (B), two (C) or several (D) neighboring holes. The scale bar is 2 nm.

Figure 3 shows the formation of two holes in a TWNT. In this case, two different atomic configurations were observed. The pristine TWNT is shown in Figure 3a, and lies on the outer part of a bundle which serves both as a support and reference frame throughout the STEM irradiation experiments. The two outermost shells of the nanotube are irradiated so that two adjacent holes appear in the outermost and the middle layer (Figure 3b). The innermost layer remains intact. Atoms with dangling bonds form interlayer bonds as in the case of DWNTs. The details of the regions are shown in the inset of Figure 3b. When all three shells are punctured with the beam (Figure 3c), another configuration is achieved, where in the middle region a 1.5 nm-wide graphene flake with two open ends is surrounded by a closed carbon shell.

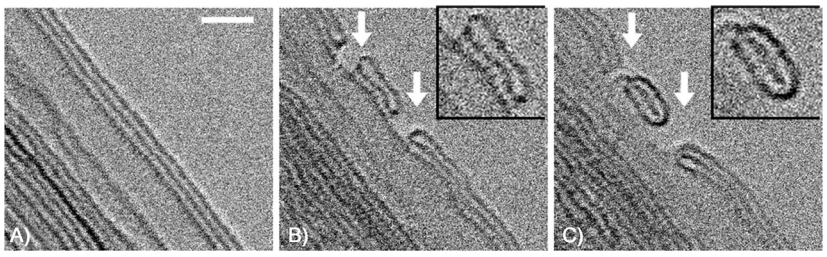

Figure 3. Formation of two holes in a TWNT: A) Before irradiation. B) The two outermost shells of the nanotube are modified to create two adjacent holes in the outermost and the middle layer. C) Three shells are punctured with the beam, leaving an isolated graphene sheet with open ends inside a closed cage. The scale bar is 2 nm.

3. Atomistic Simulations of DWNTs and TWNTs with Holes in the Layers

To understand the atomic structure of DWNTs and TWNTs with holes in the layers, we carried out atomistic computer simulations of MWNTs with a certain number of atoms being removed from the walls, similar to the experiments. As the experimental systems consist of thousands of atoms, and both short-range covalent and long-range van der Waals (vdW) interactions should be taken into account, we could not employ the proper first-principle approach[39] due to computational limitations. Instead, we used the adaptive intermolecular reactive empirical bond order (AIREBO) potential[40] which is an extension to the well-known Brenner potential.[41] The AIREBO potential is not just a sum of a short-range covalent potential and a pairwise long-range vdW term: atoms in the system are not constrained to remain attached to specific neighbors nor to maintain a particular hybridization. Depending on the local atom environment and atom separation, the long-range interaction is switched on and off, enabling the simulation of chemical reactions and defect configurations for which the interplay between covalent and long-range interactions is important. The AIREBO model has been successfully applied before to simulations of MWNTs with interlayer defects[42,43] and nanotube bundles with intertube covalent bonds.[9]

Our simulations were aimed to find the most probable atomic geometry, not at modeling the irradiation process. The response of nanotubes to electron irradiation has extensively been modeled before.[30,44] It is well known that impacts of energetic electrons give rise to the formation of vacancies[45] in the CNT walls, along with adatoms/interstitials[46] which are mobile, especially in the inner hollow of the CNTs.[34] Several DWNTs were constructed from zigzag SWNTs with diameters (3–5 nm) close to the ones observed in the experiments. The diameter of the shells was chosen to match the interlayer separation (about 0.32 nm) reported for MWNTs.[47] The atoms under the beam (Figure 1) were removed and the atomic structure was fully optimized to find a local minimum using the conjugate gradient algorithm.

We found that undercoordinated atoms in the adjacent shells of the DWNT easily form interlayer covalent bonds as shown in Figure 4a. Ultimately, two bonding configurations are possible, provided that the positions of the atoms in different shells in the upper part of the DWNT approximately match each other: "perfect" merging of the shells (Figure 4b) and bonding through carbyne-type atoms (Figure 4c). We note that the structures presented in Figures 4b–d are two merged graphene layers, but they explain quite well the more complicated morphology of the DWNT. The former configuration is lower in energy, but when there is a mismatch between atom positions, the latter configuration can be close in energy to the first one. The configurations presented in Figures 4b,c can be understood as bonding at the edges of a graphene bilayer (which can also be referred to as a fold)[36] and as bonding through interstitial-type defects[48] accumulated at the edge of the bilayer, respectively. Figure 4d shows a side view of the edge of bilayer graphene, illustrating a local "swelling" of the

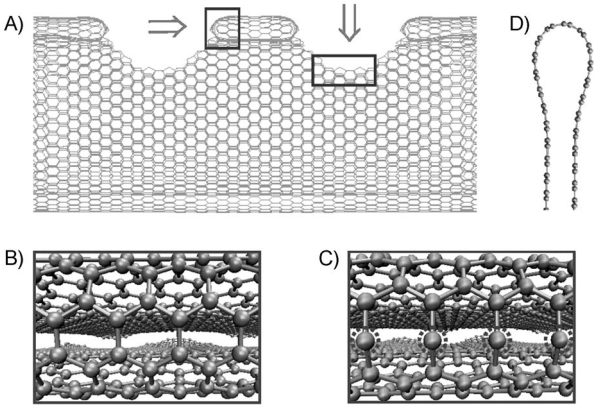

Figure 4. Atomistic model of a DWNT with atoms removed by the electron beam (A), to be compared with the experimental image in Figure 2. The atoms at the edges of the shells form covalent bonds. Ultimately, two bonding configurations are possible, provided the positions of the atoms in the different shells of the upper part of the nanotube approximately match each other: "perfect" merging of the shells (B), and bonding through carbyne-type atoms (C). The structure is locally expanded, as at the edge of the graphene bilayer in (D). The incorporation of pentagons and other non-hexagonal rings to account for curvature is also possible.

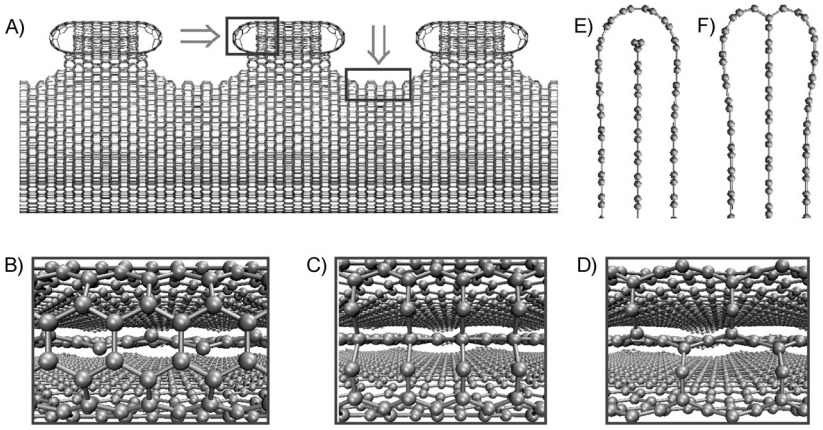

Figure 5. Atomistic model of a TWNT with atoms removed by the electron beam (A), to be compared with the experimental image in Figure 3. Atoms at the edges of the outermost and inner shells make covalent bonds, while the inner shell contains atoms with dangling bonds. In the case of three-layer graphene, three different bonding configurations are possible, as sketched in (B–D) and (E, F). Side views: a perfect fold encapsulating a flake with dangling bonds (B), and two structures with carbyne-like links between the shells. The side views of the corresponding graphene structures are presented in (E) and (F), with (E) corresponding to the configuration presented in (B), and (F) corresponding to the configurations shown in (C) and (D). The configuration with dangling bonds has the lowest energy among all, even without saturation of the dangling bonds in the middle layer with hydrogen atoms.

structure. Incorporation of pentagons and other non-hexagonal rings to account for curvature is also possible. As evident from Figure 4a, the simulated structure is in reasonable agreement with that observed in our experiments. Depending on the nanotube diameters and mutual position, both types of bonding are possible in the middle part of the cut. Under-coordinated atoms with dangling bonds that are most likely passivated with hydrogen may also exist.

Having analyzed the atomic configurations of locally merged shells in the DWNTs, we now turn to TWNTs. An atomistic model of a TWNT with atoms removed by the electron beam is presented in Figure 5. Simulations similar to those carried out for DWNTs showed that three different bonding configurations are possible, as sketched in Figure 5: a perfect fold encapsulating a shell with dangling bonds and two structures with carbyne-like links between the shells. The side views of the corresponding graphene structures are presented in Figures 5e,f, with Figure 5e showing the configuration presented in Figure 5b, and Figure 5f corresponding to the configurations shown in Figures 5c,d. In agreement with the experimental observations, our simulations showed that the configuration with dangling bonds has the lowest energy among all, even without saturation of the dangling bonds in the middle layer with hydrogen atoms. Although dangling bonds are not energetically favorable, the loss in energy is compensated by a perfect graphene envelope and avoiding carbyne-type bonds. Similar to the case of DWNTs, depending on the tube diameters and mutual position, all types of bonding are possible in the middle part of the cut. For sp^2 bonding, incorporation of pentagons and other non-hexagonal rings to account for curvature is possible.

As dangling bond atoms at the edges normally give rise to localized magnetic moments,[49,50] our results indicate that arrays of magnetic quantum dots may potentially be produced in CNTs by spatially localized electron irradiation. Further ab initio studies should clarify the behavior of magnetic moments in these systems at finite temperatures, as well as the interaction of magnetic moments at different dots.

3. Conclusions

In conclusion, we have shown that holes (of 1–3 nanometers in diameter) produced in CNTs with an electron beam display different atomic morphologies at the edge of the hole, depending on the number of CNT layers. In particular, for three holes in triple-shell structures (odd numbers), dangling bonds at the middle layer can be created and shielded by nanoarches produced by the merged outermost and innermost shells. This kind of closure should also be expected in graphene nanopores with different number of layers.

Acknowledgements

This work was supported by the Academy of Finland through the Centre of Excellence COMP and other projects and by the French Agence Nationale de Recherche (NANOCONTACTS, NT09 507527). We also acknowledge the Finnish IT Center for Science for generous grants of computer time. We are also indebted to COST Action MP0901 NanoTP for support.

Keywords: atomistic simulations · carbon · defects · electron microscopy · nanotubes

[1] A. V. Krasheninnikov, F. Banhart, *Nat. Mater.* **2007**, *6*, 723.
[2] F. Banhart, *Nanoscale* **2009**, *1*, 201.
[3] A. V. Krasheninnikov, K. Nordlund, *J. Appl. Phys.* **2010**, *107*, 071301.
[4] N. Zhichun, I. Ahmad, Y. Long, G. Jinlong, Z. Dezhang, *J. Phys. D* **2009**, *42*, 075408.
[5] D.-H. Kim, H.-S. Jang, C.-D. Kim, D.-S. Cho, H.-D. Kang, H.-R. Lee, *Chem. Phys. Lett.* **2003**, *378*, 232–237.
[6] C. Miko, M. Milas, J. W. Seo, E. Couteau, N. Barisic, R. Gaal, L. Forro, *Appl. Phys. Lett.* **2003**, *83*, 4622–4624.
[7] V. Skákalová, A. B. Kaiser, S. Roth, *Phys. Status Solidi* **2008**, *2*, 62–64.
[8] A. Kis, G. Csanyi, J. P. Salvetat, T.-N. Lee, E. Couteau, A. J. Kulik, W. Benoit, J. Brugger, L. Forro, *Nat. Mater.* **2004**, *3*, 153–157.
[9] M. Sammalkorpi, A. V. Krasheninnikov, A. Kuronen, K. Nordlund, K. Kaski, *Nucl. Instrum. Methods Phys. Res. Sect. B* **2005**, *228*, 142–145.
[10] B. Peng, M. Locascio, P. Zapol, S. Li, S. L. Mielke, G. C. Schatz, H. D. Espinosa, *Nat. Nanotechnol.* **2008**, *3*, 626–631.
[11] V. Skákalová, A. B. Kaiser, Z. Osváth, G. Vértesy, L. P. Biró, S. Roth, *Appl. Phys. A* **2008**, *90*, 597–602.
[12] J. A. Åström, A. V. Krasheninnikov, K. Nordlund, *Phys. Rev. Lett.* **2004**, *93*, 215503.
[13] Z. Ni, Q. Li, L. Yan, J. Gong, D. Zhu, *Carbon* **2008**, *46*, 376–378.
[14] M. S. Raghuveer, P. G. Ganesan, J. D. Arcy-Gall, G. Ramanath, M. Marshall, I. Petrov, *Appl. Phys. Lett.* **2004**, *84*, 4484–4486.
[15] A. V. Krasheninnikov, K. Nordlund, J. Keinonen, F. Banhart, *Phys. Rev. B* **2002**, *66*, 245403.
[16] M. Terrones, F. Banhart, N. Grobert, J. C. Charlier, H. Terrones, P. M. Ajayan, *Phys. Rev. Lett.* **2002**, *89*, 075505.
[17] J. A. Rodríguez-Manzo, A. Tolvanen, A. V. Krasheninnikov, K. Nordlund, A. Demortiere, F. Banhart, *Nanoscale* **2010**, *2*, 901–905.
[18] J. A. Rodríguez-Manzo, F. Banhart, M. Terrones, H. Terrones, N. Grobert, P. M. Ajayan, B. G. Sumpter, V. Meunier, M. Wang, Y. Bando, D. Golberg, *Proc. Natl. Acad. Sci. USA* **2009**, *106*, 4591–4595.
[19] F. Banhart, J. Kotakoski, A. V. Krasheninnikov, *ACS Nano* **2011**, *5*, 26–41.
[20] J. Kotakoski, A. V. Krasheninnikov, U. Kaiser, J. C. Meyer, *Phys. Rev. Lett.* **2011**, *106*, 105505.
[21] M. T. Lusk, L. D. Carr, *Phys. Rev. Lett.* **2008**, *100*, 175503.
[22] D. Teweldebrhan, A. A. Balandin, *Appl. Phys. Lett.* **2009**, *94*, 013101.
[23] D. W. Boukhvalov, M. I. Katsnelson, *Nano Lett.* **2008**, *8*, 4373–4379.
[24] O. Cretu, A. V. Krasheninnikov, J. A. Rodríguez-Manzo, L. Sun, R. M. Nieminen, F. Banhart, *Phys. Rev. Lett.* **2010**, *105*, 196102.
[25] J. A. Rodríguez-Manzo, O. Cretu, F. Banhart, *ACS Nano* **2010**, *4*, 3422–3428.
[26] L. Sun, A. V. Krasheninnikov, T. Ahlgren, K. Nordlund, F. Banhart, *Phys. Rev. Lett.* **2008**, *101*, 156101.
[27] L. Sun, F. Banhart, A. V. Krasheninnikov, J. A. Rodríguez-Manzo, M. Terrones, P. M. Ajayan, *Science* **2006**, *312*, 1199–1202.
[28] A. Misra, P. Tyagi, M. Singh, D. S. Misra, J. Ghatak, P. V. Satyam, D. K. Avasthi, *Diamond Relat. Mater.* **2006**, *15*, 300–303.
[29] W. S. Brian, E. L. David, *J. Appl. Phys.* **2001**, *90*, 3509–3515.
[30] A. V. Krasheninnikov, F. Banhart, J. X. Li, A. S. Foster, R. M. Nieminen, *Phys. Rev. B* **2005**, *72*, 125428.
[31] J. H. Warner, F. Schäffel, G. Zhong, M. H. Rümmeli, B. Büchner, J. Robertson, G. A. D. Briggs, *ACS Nano* **2009**, *3*, 1557–1563.
[32] A. Zobelli, A. Gloter, C. P. Ewels, C. Colliex, *Phys. Rev. B* **2008**, *77*, 045410.
[33] Ç. Ö. Girit, J. C. Meyer, R. Erni, M. D. Rossell, C. Kisielowski, L. Yang, C.-H. Park, M. F. Crommie, M. L. Cohen, S. G. Louie, A. Zettl, *Science* **2009**, *323*, 1705–1708.
[34] Y. Gan, J. Kotakoski, A. V. Krasheninnikov, K. Nordlund, F. Banhart, *New J. Phys.* **2008**, *10*, 023022.
[35] J. Kotakoski, J. C. Meyer, S. Kurasch, D. Santos-Cottin, U. Kaiser, A. V. Krasheninnikov, *Phys. Rev. B* **2011**, *83*, 245420.

[36] Z. Liu, K. Suenaga, P. J. F. Harris, S. Iijima, *Phys. Rev. Lett.* **2009**, *102*, 015501.
[37] S. Rotkin, Y. Gogotsi, *Mater. Res. Innovations* **2002**, *5*, 191 – 200.
[38] O. Lehtinen, T. Nikitin, A. V. Krasheninnikov, L. Sun, F. Banhart, L. Khriachtchev, J. Keinonen, *New J. Phys.* **2011**, *13*, 073004.
[39] A. Gulans, A. V. Krasheninnikov, M. J. Puska, R. M. Nieminen, *Phys. Rev. B* **2011**, *84*, 024114.
[40] S. J. Stuart, A. B. Tutein, J. A. Harrison, *J. Chem. Phys.* **2000**, *112*, 6472 – 6486.
[41] D. W. Brenner, *Phys. Rev. B* **1990**, *42*, 9458 – 9471.
[42] M. Huhtala, A. V. Krasheninnikov, J. Aittoniemi, S. J. Stuart, K. Nordlund, K. Kaski, *Phys. Rev. B* **2004**, *70*, 045404.
[43] S. K. Pregler, T. Hayakawa, H. Yasumatsu, T. Kondow, S. B. Sinnott, *Nucl. Instrum. Methods Phys. Res. Sect. B* **2007**, *262*, 240 – 248.
[44] F. Banhart, J. X. Li, A. V. Krasheninnikov, *Phys. Rev. B* **2005**, *71*, 241408.
[45] A. V. Krasheninnikov, *Solid State Commun.* **2001**, *118*, 361 – 365.
[46] A. V. Krasheninnikov, K. Nordlund, P. O. Lehtinen, A. S. Foster, A. Ayuela, R. M. Nieminen, *Carbon* **2004**, *42*, 1021 – 1025.
[47] *Carbon Nanotubes: Synthesis Structure, Properties and Applications* (Eds.: M. S. Dresselhaus, G. Dresselhaus, P. Avouris), Springer, Berlin, **2001**.
[48] E. Cruz-Silva, A. R. Botello-Méndez, Z. M. Barnett, X. Jia, M. S. Dresselhaus, H. Terrones, M. Terrones, B. G. Sumpter, V. Meunier, *Phys. Rev. Lett.* **2010**, *105*, 045501.
[49] Y.-W. Son, M. L. Cohen, S. G. Louie, *Nature* **2006**, *444*, 347 – 349.
[50] W. Fang, K. Erjun, X. Hongjun, W. Su-Huai, W. Myung-Hwan, Y. Jinlong, *Appl. Phys. Lett.* **2009**, *94*, 223105.

Received: December 14, 2011
Published online on March 12, 2012

